Hot And Cool: Bridging Gaps in Massive Star Evolution
ASP Conference Series, Vol. xxx, 2009
C. Leitherer, Ph. D. Bennett, P. W. Morris & J. Th. van Loon, eds.

Tidal Flows from Asynchronous Rotation in Binaries

Gloria Koenigsberger

Instituto de Ciencias Físicas, Universidad Nacional Autónoma de México, Cuernavaca, Mor., 62210, Mexico

Edmundo Moreno

Instituto de Astronomía, Universidad Nacional Autónoma de México, Mexico D.F, 04510, Mexico

David Harrington

Institute for Astronomy, University of Hawaii, 2680 Woodlawn Drive, Honolulu, HI, 96822, USA

Abstract. Asynchronous rotation in binary stars produces non-radial oscillations that are known to cause observable variability on orbital timescales. The horizontal perturbations of the surface velocity fields are referred to as "tidal flows". In this paper we illustrate the manner in which tidal flows perturb the surface velocity field from that of uniform rotation, using a one-layer stellar model for the calculations. We justify the validity of this simplified model by the striking similarity between the photospheric absorption line-profiles it predicts and observational data of the binary system α Virginis. The velocity perturbations are used to compute the mechanical energy dissipation rates, $\dot{E}$, due to the shearing flows for the case of a massive (50+28 $M_\odot$) binary system having a moderately eccentric (e =0.3) orbit. The largest value of $\dot{E}$ around periastron phases is found on the hemisphere facing the companion. However, at other orbital phases the maximum $\dot{E}$ may migrate towards the poles. Assuming that $\dot{E}$ plays a role in the mass-loss characteristics of massive binary systems, this suggests that peculiar binaries such as HD 5980 and η Carinae may have a highly non-spherically symmetric mass-loss distribution which, in addition, is time-variable.

Asynchronous rotation

A system is in synchronous rotation when the angular velocity of orbital motion Ω equals the angular velocity of the star's rotation ω_0. In eccentric orbits, the degree of synchronicity varies with orbital phase. We use periastron passage as the reference point for defining the synchronicity parameter $\beta_{per} = \omega_0/\Omega_{per} = 0.02 P v_{rot}(1-e)^{3/2} R_1^{-1}(1+e)^{-1/2}$, where e is the orbital eccentricity, the rotation velocity v_{rot} is given in km/s, the orbital period P is given in days, and the stellar equilibrium radius R_1 is given in solar units. Non-radial oscillations are excited when at any orbital phase $\beta \neq 1$. The resulting surface velocity field consists of a pattern of perturbations superposed on the unperturbed stellar rotation field. We refer to the horizontal components of the velocity perturbations, ΔV_φ, as

"tidal flows". A didactic manner of viewing the tidal flows is to imagine that due to the perturbations, some portions of the surface may be rotating slightly faster than the average rotation rate while other portions may be rotating slightly slower. The size and distribution of these "portions" depend on the modes in which the star is oscillating.

A huge body of research exists on the topic of tidal interactions, starting with Darwin (1879, 1880). References and very interesting discussions may be found in Eggleton et al. (1998) and Ferraz-Mello et al. (2008). However, the focus is generally on the long-term evolution of the orbital parameters. We in turn focus on the short-term effects, especially those that may influence the observational properties of stars on orbital timescales.

Our method consists of computing the motion of a Lagrangian grid of surface elements distributed along a series of parallels (i.e., rings with different polar angles) covering the surface of a star of mass M_1 as it is perturbed by its companion of mass M_2. The main stellar body below the perturbed layer is assumed to be in uniform rotation. The equations of motion that are solved for the set of surface elements include the gravitational fields of M_1 and M_2, the Coriolis force, and the gas pressure. The motions of all surface elements are coupled through the viscous stresses included in the equations of motion. The kinetic energy of the tides may be dissipated through viscous shear, thus leading to an energy dissipation rate, $\dot{E}$. The rate of energy dissipation per unit volume is given by the matrix product $\dot{E} = -\mathbf{P}_\eta : \nabla \boldsymbol{v}$, where $\mathbf{P}_\eta$ is the viscous part of the stress tensor and $\boldsymbol{v}$ is the velocity of a volume element with respect to the center of the star (for details see Moreno & Koenigsberger 1999; Moreno et al. 2005; and Toledano et al. 2007).

The benefits of our method are: 1) we make no *a priori* assumption regarding the mathematical formulation of the tidal flow structure since we derive the velocity field $\boldsymbol{v}$ from first principles; 2) the method is not limited to slow stellar rotation rates nor to small orbital eccentricities; and 3) it is computationally inexpensive and contains only two free parameters, the viscosity and the thickness of the surface layer.

Surface Velocity Field and Energy Dissipation rates

In Figure 1 we illustrate the characteristics of the perturbations of the azimuthal velocity field, ΔV_φ at periastron passage for a M_1+M_2 =50+28 $M_\odot$ binary system with P=19.3 d, e=0.3 and R_1=21 $R_\odot$. Shown is the hemisphere containing the sub-binary longitude, φ =0. The corresponding values of ΔV_φ on the equatorial latitude are plotted in the right panel, illustrating the alternating positive and negative nature of this field. The largest perturbation in the direction of stellar rotation occurs slightly west of the sub-binary longitude. The largest perturbation in the opposite direction occurs at a longitude of $\sim 60^\circ$.

The shear energy dissipation rate $\dot{E}$ depends on the absolute value of the velocity perturbations, thus its azimuthal distribution has twice as many maxima and minima. A map of $\dot{E}$ corresponding to the velocity field displayed in Figure 1 is in Figure 2 (left), with the corresponding plot for the equatorial latitude (right). Since $\dot{E}$ is a function of ΔV_φ, energy dissipation rates are large wherever the absolute value of the azimuthal velocity is large.

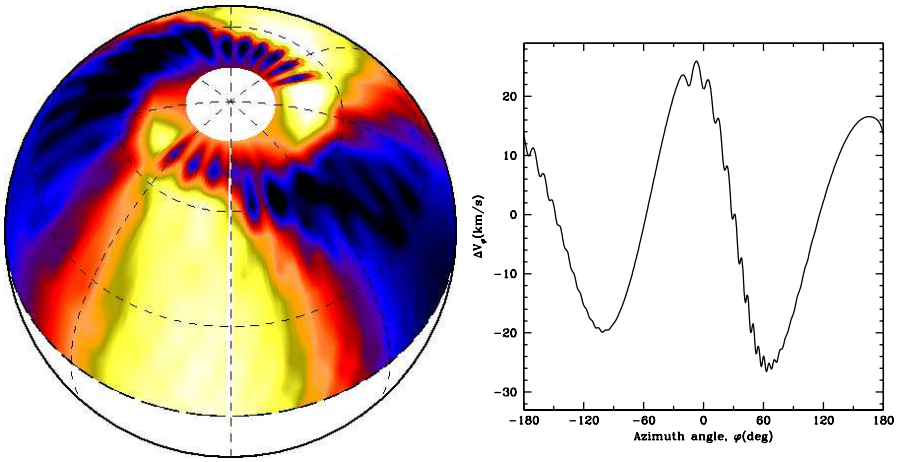

Figure 1. Left: Distribution of the azimuthal velocity perturbations, ΔV_φ, at periastron passage for the 50+28 $M_\odot$ model discussed in the text. Color scale is such that white indicates maximum perturbation in the direction of rotation while black indicates maximum perturbation in the opposite direction. The sub-binary longitude is the vertical line in the middle of the map; the rotation axis is tilted with respect to the plane of the paper by 55°. Right: Plot of ΔV_φ for the equatorial latitude, where positive values correspond to perturbations in the direction of rotation.

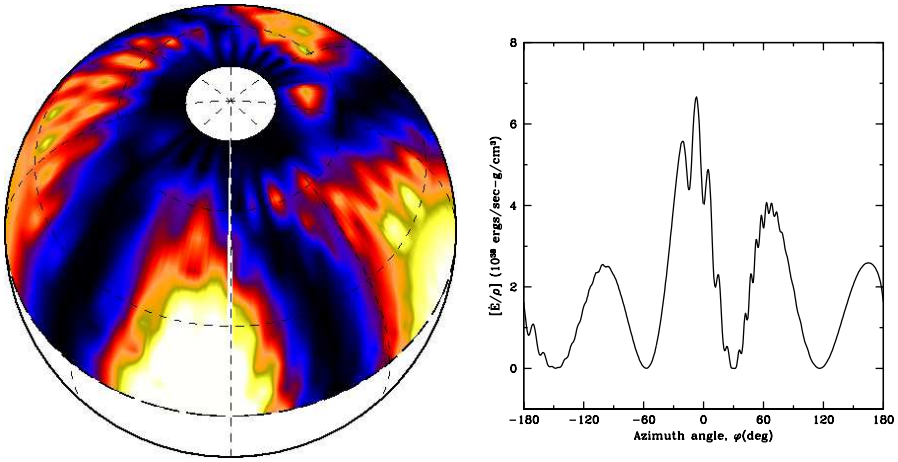

Figure 2. Same as previous figure except that here we illustrate the distribution of the energy dissipation rate, $\dot{E}$, and the color scale such that white indicates maximum $\dot{E}$ and black indicates minimum values.

It is interesting to follow the changes over the orbital cycle in the $\dot{E}$ distribution. A selection of orbital phases is illustrated in Figure 3 for the same binary system displayed in Figures 1 and 2. The maps are oriented so as to show the longitude range that would be visible to an observer at the given orbital phases. Shortly after periastron (ϕ =0.10, bottom right), the pattern remains similar to that shown in Figure 2 (periastron), although the actual values of $\dot{E}$ are larger. As the star approaches apastron, the values rapidly decrease and the pattern of maximum $\dot{E}$ breaks down into smaller zones and migrates towards the poles. After apastron, the zones of large $\dot{E}$ begin to grow once again and migrate towards the equator.

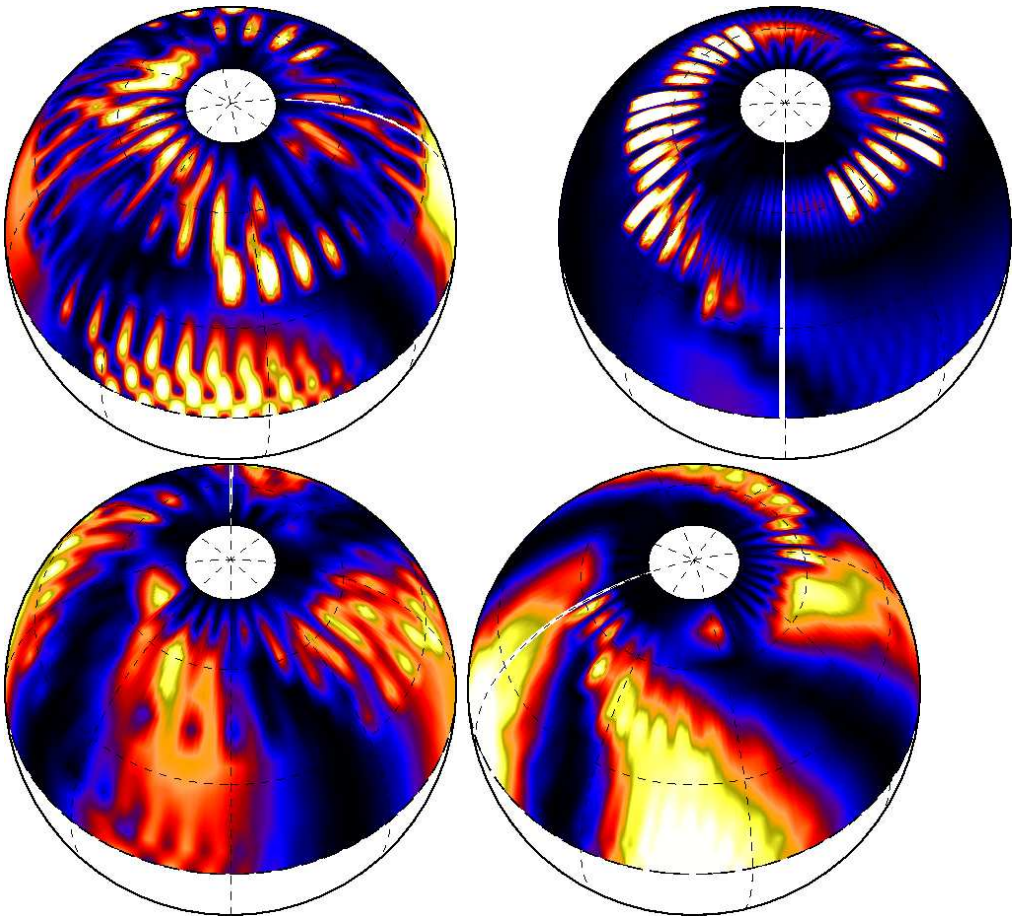

Figure 3. Orbital phase-dependence of the $\dot{E}$ distribution over the stellar surface for the same model illustrated in Figures 1 and 2 for phases with respect to periastron passage as follows: 0.10 (bottom right), 0.30 (top right) and 0.80 (top left) and 0.95 (bottom left). The maps are oriented so as to show the range in longitudes that would be visible to an external observer and color coding is the same as in Figure 2.

Photospheric line-profile variability

A natural question that arises concerns the validity of the one-layer approximation upon which our model is currently based. One way to address this issue is by comparing the model results with observations of photospheric absorption line-profile variability.

Figure 4 illustrates the Si III 4552 Å absorption line observed at four different orbital phases in the B-type binary system α Virginis (Spica; P=4.01 days, e=0.1). The observations were performed at the Canada France Hawaii (CFHT) 3.6m telescope with the ESPaDOns spectropolarimeter at a nominal spectral resolution of R=68,000 on 2008 March 20–28 (Harrington et al. 2009, in Preparation). The variability consists primarily of the presence of "bumps" on the line profile that systematically change their location over time, as was first studied in detail by Smith (1985a, 1985b) is clearly seen. Noteworthy also is the "boxy" shape of the absorption at some orbital phases. The dotted lines superposed on the observations correspond to the theoretical line profiles computed with our model for the corresponding orbital phases. The model reproduces both the general shape of the observational data as well as the number and location of "bumps". Since this model is computed directly from first principles with only the single-layer approximation as an assumption and with very few free parameters, the similarity between the computed and observed line profiles is striking. The reason why the one-layer approximation works so well in this case is that the dominant effect producing the line profile variability arises from the external gravitational perturbation, rather than from the star's internal oscillation modes.

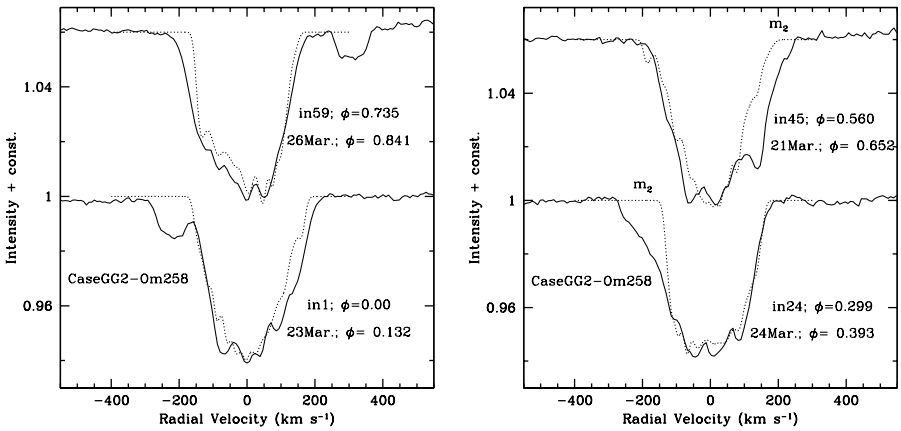

Figure 4. Comparison of observations with theoretical (dots) line profiles for 4 orbital phases in the binary systems α Virginis (Spica). Note that the one-layer model yields line profiles with a general shape that is similar to that of the observations, and that the number and location of the sub-peaks also coincide. The absorption line from the lower-mass companion is clearly visible in the left panel, but in the right panel it blends with the primary's absorption. Its location is indicated by the label "m_2" and accounts for the larger discrepancy between the observed and theoretical profiles in the right panel.

Tidal flows and surface activity

Although synchronous rotation is generally assumed for the analysis of a large variety of binary systems, the uncertainties in the stellar radius, rotational velocity and orbital inclination generally allow for significant departures from the assumed corrotating state. Furthermore, no star in an eccentric orbit is in synchronous rotation. Hence, the presence of tidal flows on the surface of binary stars is likely to be much more prevalent than generally assumed.

Tidal flows produce a surface velocity field having gradients in both the azimuthal and polar directions. In addition, due to the radial dependence of tidal forces, the velocity amplitudes on the surface are larger than those in internal regions, hence also creating a rotation velocity gradient in the radial direction. All these gradients are strongly time-dependent. We suggest that the strong and rapid variations in these gradients may lead to a much larger degree of turbulence on the stellar surface than is present in synchronized binaries or single stars. It is also tempting to speculate that these effects could potentiate the appearance of localized magnetic fields (Ulmschneider & Musielak 1998).

Tidal flows lead to energy dissipation due to the associated viscous shear. The additional energy in surface layers could conceivably alter the radial temperature gradient as well as produce a non-uniform effective temperature distribution over the stellar surface. It is interesting to speculate on the possible effect that this additional energy source could produce on stellar winds. For example, since the tidal shear is not uniformly distributed over the stellar surface, the question arises as to whether $\dot{E}$ can contribute towards enhancing the mass-loss rate. Alternatively, localized magnetic fields or surface convective regions might tend to inhibit the radiatively-driven outflows at the base of the wind. Hence, in extreme cases where $\dot{E}$ is significant, our model would predict a highly non-spherically symmetric mass-loss rate. In addition, the asymmetry would be greatest near periastron passage, with a wind whose characteristics are dominated by the strong perturbations near the equatorial latitudes while near aperiastron the effects of the perturbation might be concentrated near the polar regions.

Acknowledgments. We are grateful to Ben Brown for providing the idl scripts used to produce Figs. 1–3. This investigation was partially supported by grants UNAM/PAPIIT 106708, CONACYT 24936 and NSF AST-0123390, the University of Hawaii and the AirForce Research Labs (AFRL).

References

Darwin, G. H., 1879 Philos. Trans. 170, 447
Darwin, G. H., 1879 Philos. Trans. 171, 713
Eggleton, P. P., Kiseleva, L. G. & Hut, P. 1998, ApJ, 499, 853
Ferraz-Mello, S., Rodríguez, A. & Hussmann, H. 2008, CeMDA, 101, 171
Moreno, E. & Koenigsberger, G. 1999, RMA&A, 35, 157
Smith, M. A. 1985a, ApJ, 297, 206
Smith, M. A. 1985b, ApJ, 297,224
Toledano, O., Moreno, E., Koenigsberger, G., Detmers, R., & Langer, N. 2007, A & A, 461, 1057
Ulmschneider, P. & Musielak, Z.E. 1998, A&A, 338, 311